ELSEVIER

Journal of Alloys and Compounds 387 (2005) 24–31

Journal of ALLOYS AND COMPOUNDS

www.elsevier.com/locate/jallcom

Raman spectroscopy of $PbTe_{1-x}S_x$ alloys

N. Romčević[a,*], J. Trajić[a], M. Romčević[a], A. Golubović[a], S. Nikolić[a], V.N. Nikiforov[b]

[a] *Institute of Physics, P.O. Box 68, 11080 Belgrade, Serbia and Montenegro*
[b] *Low-temperature Physics Department, Moscow State University, 119899 Moscow, Russia*

Received 8 March 2004; received in revised form 17 June 2004; accepted 17 June 2004

Abstract

Raman scattering spectra as well as results of galvanomagnetic, X-ray and ultrasonic measurements of $PbTe_{1-x}S_x$ (x = 0.02 and 0.05) mixed crystals in the temperature range from 10 to 300 K are presented. A structural phase transition at about T_c = 60 K for x = 0.05 was detected, whereas for samples with x = 0.02, the phase transition was not observed. The two TO/LO mode pairs of $PbTe_{1-x}S_x$ mixed crystals are determined from Raman spectra at all temperatures, and according to that we found that the optical phonon modes of these mixed crystals showed a two-mode behaviour. The model of phonon behaviour based on the model of Genzel et al. was applied. One additional mode, at about 75 cm^{-1}, the intensity of which is connected with off-center sulphur ions, is observed in all samples. Our results suggest that the only reason for complex phase transition in $PbTe_{1-x}S_x$ systems may be the off-center sulphur ions.
© 2004 Elsevier B.V. All rights reserved.

Keywords: Impurities in semiconductors; Ultrasonics; X-ray diffraction; Light absorption and reflection

1. Introduction

The low-temperature ferroelectric phase transition is an interesting feature of some IV–VI semiconductors. Two different approaches have been proposed to explain the appearance of ferroelectricity in IV–VI semiconductors: the ferroelectric phase transition in GeTe, SnTe and $Pb_{1-x}Sn_xTe$ was explained by the softening of TO-mode at gamma point of the Brillouin zone [1,2], while the transition in $Pb_{1-x}Ge_xTe$ was attributed to the ordering of dipoles formed by off-center ions [3,4].

$PbTe_{1-x}S_x$ is a narrow gap semiconductor with a direct gap in the infrared domain [5]. Recent experimental studies [5–8], indicate that there is a second-order phase transition in the $PbTe_{1-x}S_x$ system. Its ferroelectric nature was proved by dielectric measurements [5]. The phase transition in the $PbTe_{1-x}S_x$ alloy system has several interesting anomalies. First, these alloys are different from the previously studied IV–VI cation-substituted solid solutions in which at least one of the end-member binary components is ferroelectric [9]. Namely, PbTe and PbS are paraelectric at all temperatures. Second, although PbTe itself is not ferroelectric, the addition of only 2% of S to PbTe induces the phase transition and, for higher concentrations, T_c is a strongly non-linear function of x. Third, the $PbTe_{1-x}S_x$ alloys may undergo a complex phase transition: a coupled orientational order–disorder and displacive ferroelectric phase transitions (FPT), where the long-range ordering of dipoles created by off-center sulphur ions may induce the bulk displacive FPT [10].

The phonon properties of $PbTe_{1-x}S_x$ are not studied yet. But it is obvious that one cannot treat $PbTe_{1-x}S_x$ alloys by simply interpolating the phonon behaviour between two end-point materials. Also, the subject of the investigation were mixed crystals with a relatively high concentration of sulphur [10]. Raman spectroscopy is a powerful technique for investigation in this field.

In our paper Raman spectra were measured on two samples of $PbTe_{1-x}S_x$: in the composition, where the phase transition is not observed (x = 0.02), and on the sample where the complex phase transition exists (x = 0.05).

* Corresponding author. Tel.: +381-11-3160-346; fax: +381-11-3161-190.
E-mail address: romcevi@phy.bg.ac.yu (N. Romčević).

0925-8388/$ – see front matter © 2004 Elsevier B.V. All rights reserved.
doi:10.1016/j.jallcom.2004.06.059

2. Experiment

Single crystals of $PbTe_{1-x}S_x$ alloys were grown by the vapour–liquid–solid (VLS) technique, using metal and chalcogenide atoms of high purity as source materials. The details of the growth procedure can be found in [5]. The chemical composition of the samples was controlled by X-ray microprobe investigation.

Characterization of the obtained samples was carried out by:

- X-ray diffraction analysis (powder diffractometer Siemens D500 with Cu K_α, Ni-filtered radiation, in the diffraction angle range $2\theta = 25$–100°);
- transport measurements: resistivity $\rho(T)$ was determined in the Van der Pauw contact geometry. The size of the samples was about 3.5 mm in diameter with a thickness of about 0.75 mm. The current through the samples was I = 10 mA;
- acoustic measurements: the sample has a disk-like form with the dimensions $1 \times 10 \times 10\,mm^3$. The direction of acoustic wave propagation was [0 0 1]. For the generation of ultrasound, the effect of direct transformation of electromagnetic waves into ultrasound waves is used [11]. Because of that, on both sample plane surfaces [0 0 1] thin conductivity aluminium layers (1 μm) were created. Applying electromagnetic waves on metal surface produces ultrasound when a constant magnetic field is present. Excitation is induced by the Lorentz interaction between the magnetic field (H_o) and the metal sample free electrons. Using this method, it is possible to excite and detect both transverse (t) and longitudinal (l) ultrasound waves, by changing the space orientation of the applied constant magnetic field. A pair of solenoids around the sample realizes excitation and detection of ultrasound oscillations. The resonance characteristics of the surface sample impedance is registered when the ultrasound waves are present in the sample is an object of the experimental observations. The resonance frequency f_n detected under standing waves on the thickness d of the installation allows the calculation of the ultrasound velocity value $S_{l,t}$. The accuracy of acoustic wave frequency ($f_{l,t} = nS_{l,t}/2d$, n = 1,3,. . .) detection is 10^{-5}. The intensity of the magnetic field during the measurements was H_o = 50 kO at the frequency $f \sim 50$ Hz.
- The Raman spectra were taken with the 514.5 nm and 488 nm lines of an Ar laser using a Dilor multichannel Raman spectrometer equipped with a liquid-nitrogen-cooled charge-coupled-device detector.

2.1. Sample characterization

The samples were cut parallel to [1 0 0] (the cleavage plane) with an inner blade diamond cutter and then mechanically polished. We did not find solutions for chemical polishing and etching of $PbTe_{1-x}S_x$ alloys in the literature. Chemical polishing was carried out with solutions of 5 vol.% Br_2 in an HBr at room temperature after exposure for 3 min. We successfully used this solution for $Pb_{1-x}Mn_xTe$ alloys [12], but the exposure time for this system was 2 min.

The widely known etch pit technique is very suitable for the study of crystalline solids. For such studies, cleavage planes are often preferred to the mature surface, because the former are free from the usual growth features and the characteristic surface marking which affects each pattern produced. As in the case for the chemical polishing, we used a mixture of 20 g KOH in 1 ml H_2O_2 at room temperature as etching solution for $PbTe_{1-x}S_x$. The exposure time was 7 min, 1 min longer than for $Pb_{1-x}Mn_xTe$ alloys [12]. The etching produced sizable pits with a characteristic shape for the [1 0 0] plane. The microscopic observation of chemically etched [1 0 0] surfaces also revealed other structural characteristics. It was confirmed that low-angle grain boundary free $PbTe_{1-x}S_x$ single crystals were obtained, and no cellular structure and metal inclusions were observed. The other structural characteristics were obtained by the XRD powder technique. The unit cells of $PbTe_{1-x}S_x$ were calculated by a least square method (presented in the insert of Fig. 1), and obey Vegard's rule [13]. Fig. 1 presents X-ray diffractograms for powdered $PbTe_{1-x}S_x$. The refracting planes are denoted by (*hkl*) indices and they correspond to literature data [JCPDS 38–1435], except the reflection at $2\theta \sim 38^\circ$ (denoted by *), which corresponds to PbS [JCPDS 20-0596]. $PbTe_{1-x}S_x$ is a pseudo-binary alloy (PbTe–PbS) with rock salt structure, and a content of 5% S can be detected by the X-ray technique.

The temperature dependencies of the resistivity $\rho(T)$ for two $PbTe_{1-x}S_x$ samples are given in Fig. 2 (denoted by o and + for x = 0.02 and 0.05, respectively). For the sample with x = 0.05 we found a local maximum in the resistivity curve at about T = 60 K, (arrow in Fig. 2) with a width ΔT = 2 K. In the boundary compounds (PbTe and PbS) [13] and in $PbTe_{0.98}S_{0.02}$ such behaviour is not observed.

The temperature dependencies of the velocity of longitudinal (S_l) and transverse (S_t) ultrasonic wave propagating along the [0 0 1] direction for the $PbTe_{0.95}S_{0.05}$ single crystal are shown in Fig. 3. Near $T \sim 60$ K there is an evident anomaly represented by an abrupt change in velocity of the longitudinal ultrasound wave ($\Delta S/S_l \sim 2.8\%$), while the change in velocity of the transverse ultrasound wave is much smaller ($\Delta S/S_t \sim 0.2\%$). The smaller anomaly, which can be seen in the curve of temperature dependency of transversal ultrasound wave velocity, is a result of the significantly smaller (two or three times) sensitivity of the displacement module on compression fluctuation near the phase transition temperature.

The registered anomaly (Figs. 2 and 3) is a result of the ferroelectric phase transition. The exact phenomena of the ferroelectric phase transition in the $PbTe_{1-x}S_x$ mixed crystals are not clearly understood yet. But, as we have already mentioned, the only reason for the registered complex phase transition and ferroelectrivity in $PbTe_{1-x}S_x$ may be the off-centering of the S atoms. An off-center site is favoured when

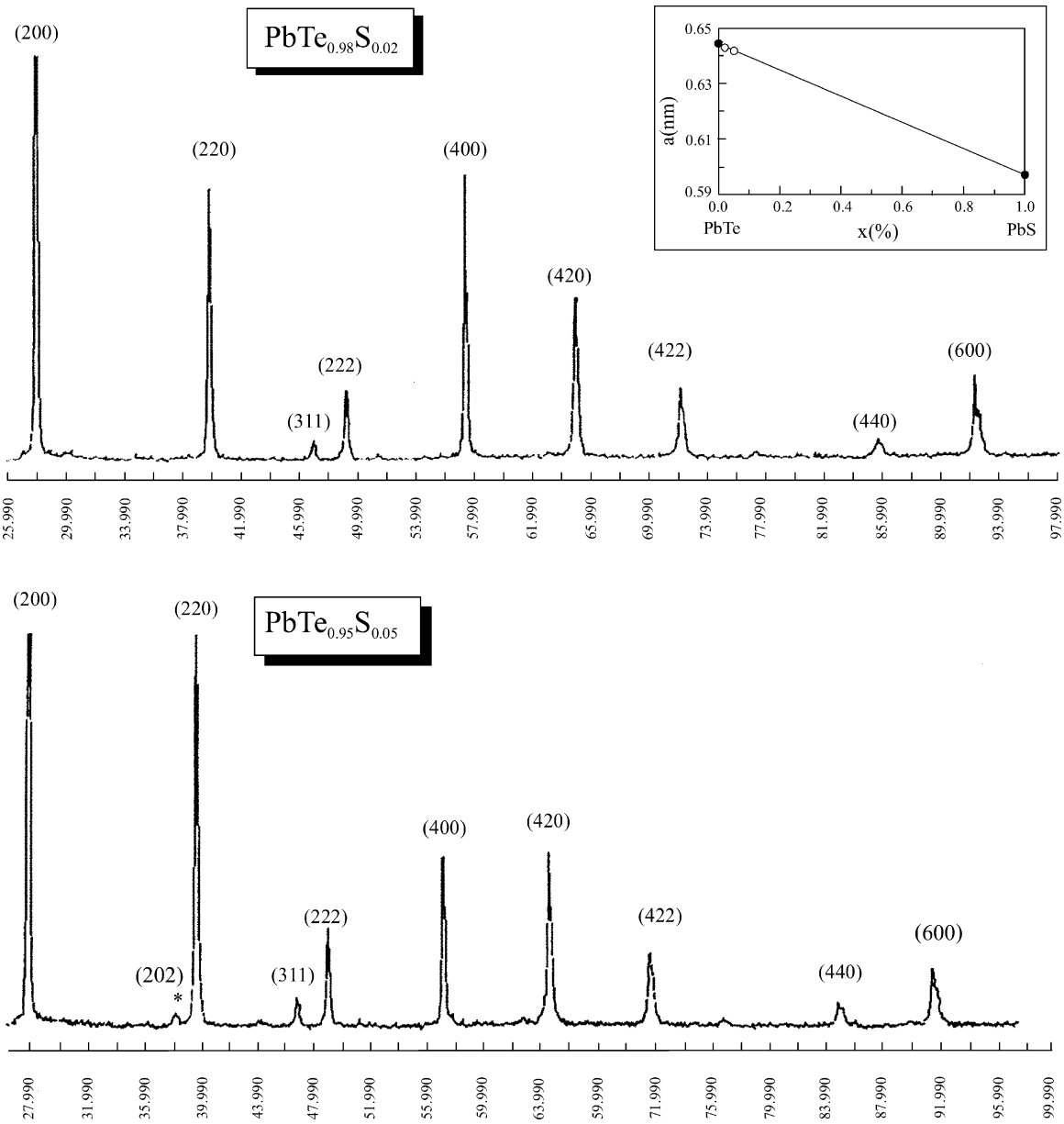

Fig. 1. X-ray diffractogram of $PbTe_{1-x}S_x$ single crystals. Inset: the lattice parameter a vs. concentration (◯). Parameters for the end members (●) were taken from [13].

a large ionic size difference causes a decrease in repulsive force because of reduced ionic overlap, and a large difference between the polarizability of an impurity ion and that of the lattice it replaces results in a decrease in polarization energy [14]. The polarization force tends to drive the impurity ion towards the neighbour ions, while the repulsive force tends to keep the impurity ion in the lattice site. The balance point of these two forces is the actual position of the impurity ion, which is off the normal lattice site position. The replacement of Te^{2-} by S^{2-} in $PbTe_{1-x}S_x$ satisfies these conditions [10]. Namely, the ionic radius of S^{2-} is 1.90 Å and that of Te^{2-} is 2.22 Å. Since the S^{2-} is about 0.32 Å smaller than Te^{2-} and the polarizability of S^{2-} is about half of that for Te^{2-} (S^{2-}: 5.0, Te^{2-}: 10.0), it is very likely that S^{2-} is displaced from the normal S^{2-} site, forming a permanent dipole. The sulphur ions are off-center in both high- and low-temperature phases. The corresponding off-center displacement of the ions depends strongly on the sulphur concentration. The magnitude of the off-center displacement of the ions is important in the physics of these materials. The larger the displacement, i.e. the larger the magnitude of the dipole moment, the stronger is its effect on the phase-transition-related properties. The off-center S ions are randomly oriented in different [1 1 1] directions in the high temperature phase. These off-center ions form local electric dipoles that undergo an orientational order–disorder

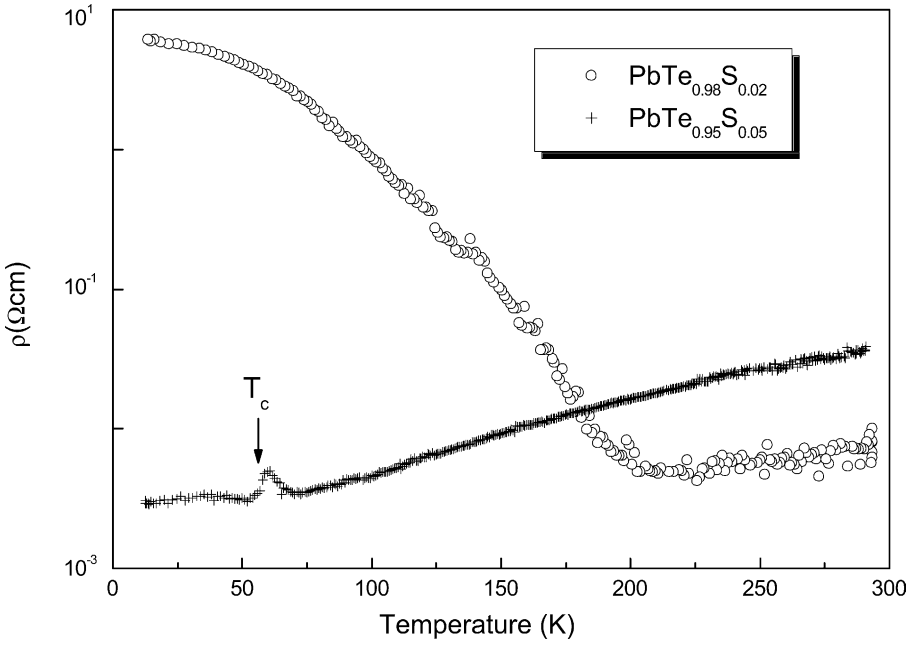

Fig. 2. Temperature dependencies of resistivity of $PbTe_{1-x}S_x$ mixed crystals.

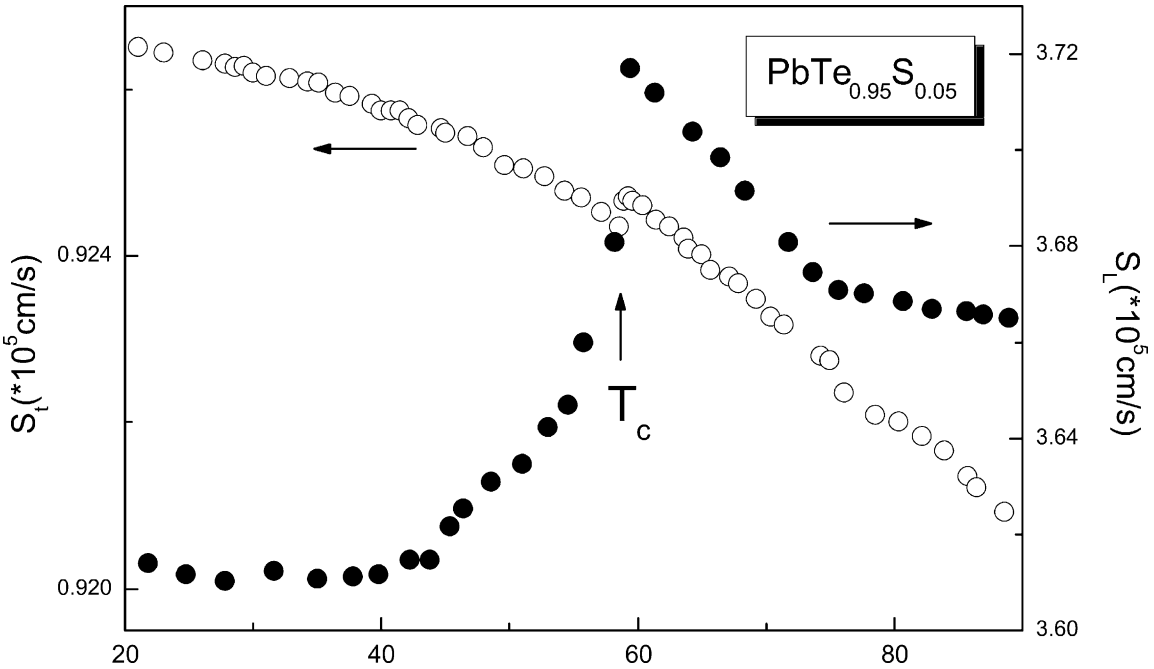

Fig. 3. Temperature dependencies of the velocity of longitudinal (S_l) and transverse (S_t) ultrasonic waves propagating along [0 0 1] direction for $PbTe_{0.95}S_{0.05}$ single crystal.

transition, which in turn may induce the displacive transition. So, this system involves an effective double-phase-transition: an order–disorder ferroelectric phase transition due to the alignment of the off-center S ions along the [1 1 1] direction, and a bulk displacive FPT along the same [1 1 1] direction [10] at temperature T_c = 60 K, for x = 0.05 in our case.

3. Raman spectra : results and discussion

The non-polarized Raman spectra of $PbTe_{1-x}S_x$ in the spectral range from 25 to 220 cm^{-1} at temperature between 20 and 300 K are shown in Fig. 4. Experimental results are presented by circles. Full lines are results of application of deconvolution, which will be described later (see Fig. 5).

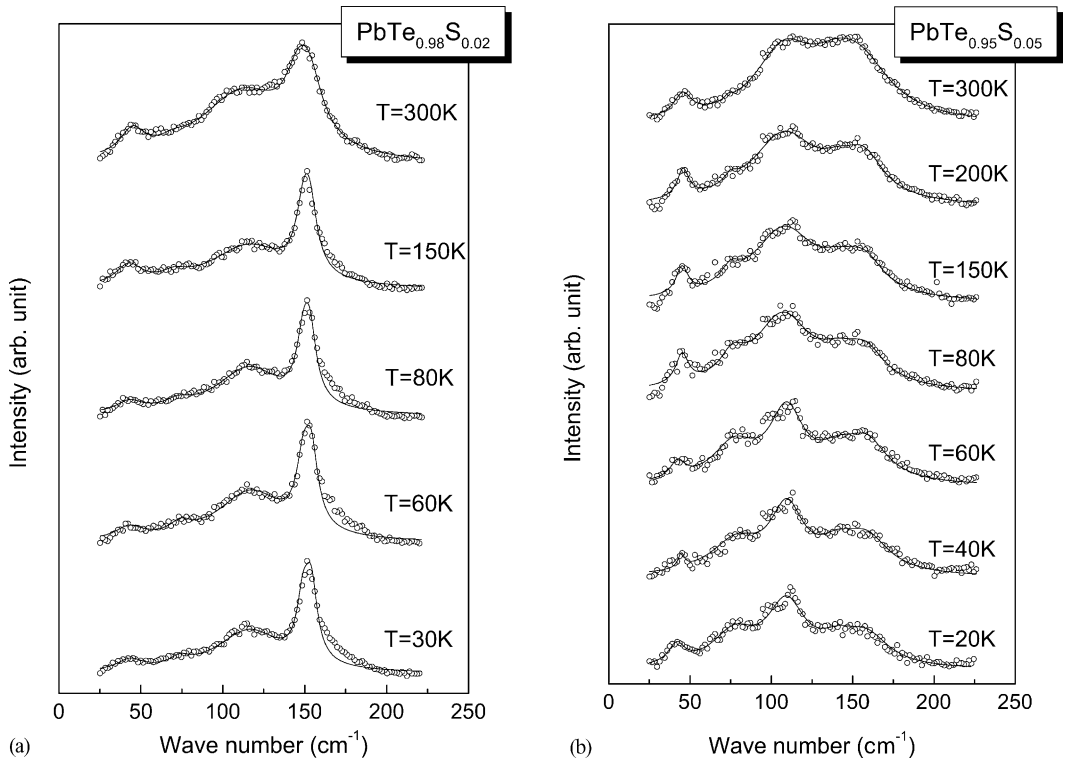

Fig. 4. Non-polarized Raman scattering spectra of $PbTe_{1-x}S_x$ mixed crystals at different temperatures: (a) $x = 0.02$; (b) $x = 0.05$.

The samples were polished just before measurement in order to prevent the formation of the TeO_2 and PbO layer. Because of that, the intensity of its mode [15] is very low. In all samples three dominant structures at about 40, 100 and 150 cm^{-1} are clearly observed. At temperatures $T <$ 100 K, an additional mode at about 75 cm^{-1} is registered in the sample with $x = 0.05$. Also, at the same temperature, the complex nature of structure at about 150 cm^{-1} is visible.

Raman spectra are often analysed with the help of a Lorentzian function or by the convolution of a Lorentzian and Gaussian curves [16,17]. As the quality of the spectra in Fig. 4 is such that it allows only a quantitative analysis with a partial discussion of the trend, we assume that all lines are of Lorentzian type. A typical line shape obtained in this way is shown in Fig. 5. This picture is characteristic for $A_{1-x}B_xC$ alloys with relatively small x [18]. In that way, we registered five lines the position and intensity of which depend on composition and temperature.

In principle, PbTe and PbS crystallize in the cubic NaCl type structure (O_h space group symmetry), and the first order Raman modes are not active. In our opinion, off-centered sulphur atoms are responsible for the Raman activity in $PbTe_{1-x}S_x$ systems. As we shall see later four of the registered modes are phonon lines and satisfy the so called two-mode behaviour, and the mode at 75 cm^{-1} is strongly connected with the ferroelectric phase transition and represents the phonon density of states of the $PbTe_{1-x}S_x$ mixed crystals.

3.1. Phonon properties of $PbTe_{1-x}S_x$ mixed crystals

In this part of the paper we applied a model for phonon mode behaviour for the ternary compound $A_{1-x}B_xC$ based on the model of Genzel et al. [19], and then check the agreement between theoretical and experimental results.

In our calculations the basic assumptions of the REI model [20] are employed. For mixed crystals of $A_{1-x}B_xC$ type they may be formulated as follows:

- the crystal lattice of a mixed system comprises two sublattices, one of them occupied by C atoms only and the second statistically occupied by A and B atoms;
- the atoms of the same kind vibrate in the same phase and with the same amplitude;
- each atom is subjected to the forces produced by the statistical average of the surrounding atoms.

If we take into account the influence of the effective electric field on the motion of the atoms in $Te_{1-x}S_xPb$, the following equations of motion for Te, S and Pb atoms could be written:

$$m_t\ddot{u}_t = -F_{tp}(u_t - u_p) - xF_{ts}(u_t - u_s) + e_{tp}E_{loc} \quad (1)$$

$$m_s\ddot{u}_s = -F_{sp}(u_s - u_p) - (1-x)F_{ts}(u_s - u_t) + e_{sp}E_{loc} \quad (2)$$

$$m_p\ddot{u}_p = -xF_{sp}(u_p - u_s) - (1-x)F_{tp}(u_p - u_t) - [(1-x)e_{tp} + xe_{sp}]E_{loc} \quad (3)$$

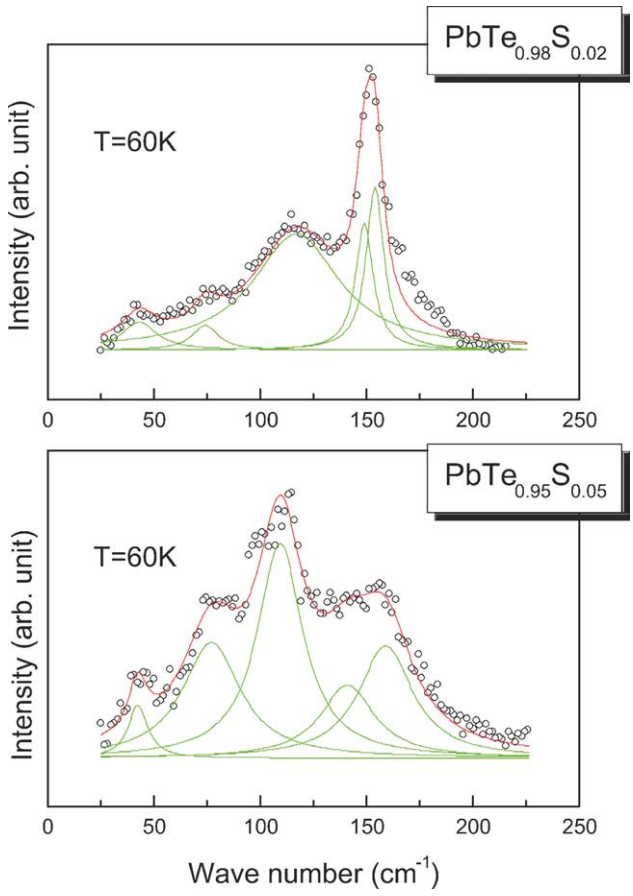

Fig. 5. The results of the application of the deconvolution on the spectrum of $PbTe_{1-x}S_x$: (a) $x = 0.02$ ($T = 60$ K), and (b) $x = 0.05$ ($T = 60$ K).

where m_t, m_s and m_p are the masses of the atoms Te, S and Pb, u_t, u_s and u_p are the displacements, F_{tp} and F_{sp} are the force constants between the nearest neighbours, F_{ts} is the force constant between the second neighbours Te and S, and e_{tp} and e_{sp} are the effective charges of the corresponding binary compounds. E_{loc} is a local electric field defined in [21];

$$E_{loc} = \frac{1}{\eta}[(1-x)e_{tp}(u_t - u_p) + xe_{sp}(u_s - u_p)] \quad (4)$$

$$\eta = v\xi - [(1-x)(\alpha_t + \alpha_p) + x(\alpha_s + \alpha_p)] \quad (5)$$

a_t, a_s and a_p are electronic polarizabilities of the ions Te, S and Pb. The volume of the primitive cell v is given by $v = a^3/4$, where a is the lattice parameter of the cubic crystals, which vary with composition: $a(x) = a_{tp} + (a_{sp} - a_{tp})x$, where a_{tp} and a_{sp} are lattice parameters of corresponding binary compounds PbTe and PbS. As we see from Fig. 1, this assumption is justified. ξ is constant, and its value is $\xi(TO) = 3/4\pi$ for transverse modes, and $\xi(LO) = -3/8\pi$ for longitudinal modes.

The microscopic parameters of Eqs. (1)–(5) are related to macroscopic parameters according to usual Born–Huang procedure [19]. We assumed that the force constant between the nearest neighbours does not vary with composition x [19]. Macroscopic parameters are given in Table 1.

Table 1
Parameters in the model for $PbTe_{1-x}S_x$

	a (10^{-10} m)	ω_{TO} (cm^{-1})	ω_{LO} (cm^{-1})	ε_0	ε_∞	Reference
PbTe	6.44	46	114	400	65.13	[13]
PbS	5.97	66	216	175	16.34	[13]

The force constants between the second neighbours were determined from impurity modes. In the case of sulphur impurity mode in PbTe, we assume its position from experiment (151 cm^{-1}). The position of Te impurity in PbS was estimated in the simplest way, which is described in detail in [22]:

$$\omega_{ITe} = \omega_{TOPbS}\sqrt{\frac{m_s}{m_t}} = 33\,cm^{-1} \quad (6)$$

The curves shown in Fig. 6 were obtained by solving Eqs. (1)–(5). The experimental values for TO and LO modes are marked by full circles (●), the values taken from literature—by full squares (■), and values for impurity modes by open circles (◯). Agreement between experimental and theoretical results is very good, with regard to the approximations on which these models are based.

The results shown in Fig. 6 suggest that the optical phonons in $PbTe_{1-x}S_x$ mixed crystals have a well-known two-mode behaviour, according to the notation of Genzel et al. [19].

3.2. Nature of the mode at 75 cm^{-1}

The temperature dependence of the mode at about 75 cm^{-1} for both samples is presented on Fig. 7. In the case of the sample with $x = 0.02$, the mode intensity is relatively low, and the changes remain within the error range with decreasing temperature. For the sample with $x = 0.05$, the intensity of this mode is low at high temperatures, and there is not significant difference from the $x = 0.02$ sample. Below about 100 K, a modest increase of the mode intensity is observed in the sample with $x = 0.05$. At $T \sim 60$ K, there is a strong increase of the mode intensity. With further temperature decrease, the increase of the mode intensity is weak and hardly noticeable. This kind of temperature dependence of the mode intensity has not been observed in the case of other PbTe based systems, as far as we know.

This mode can not be the sulphur local mode, because if the semiconductor is doped with a substitutional impurity [23] (in this case sulphur), and when the substitution involves the atoms of lighter mass (in this case Te), a lighter impurity leads to a localized mode which rises out of the top of the optical band. As we see from Fig. 6 the position of this mode is about 151 cm^{-1}. But, the influence of the impurity may be seen as amplification of the host crystal mode intensities, which are in some way forbidden (by the selection rules, or these are second order modes, etc.), whereas the mentioned modes have definite phonon state density. The mode position observed at about 75 cm^{-1} is equal to the Brillouin zone edge

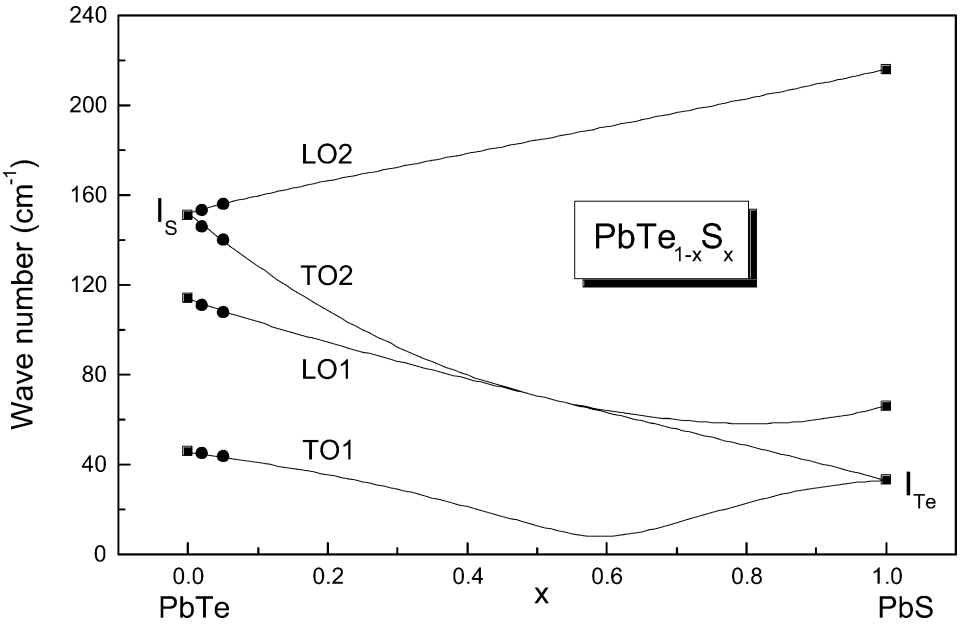

Fig. 6. Concentration dependence of the optical mode frequencies of $PbTe_{1-x}S_x$ single crystals; full circles stand for the experimental results; full squares are values taken from the literature; open circles and solid lines are obtained by the model described in this paper (Eqs. (1)–(6)).

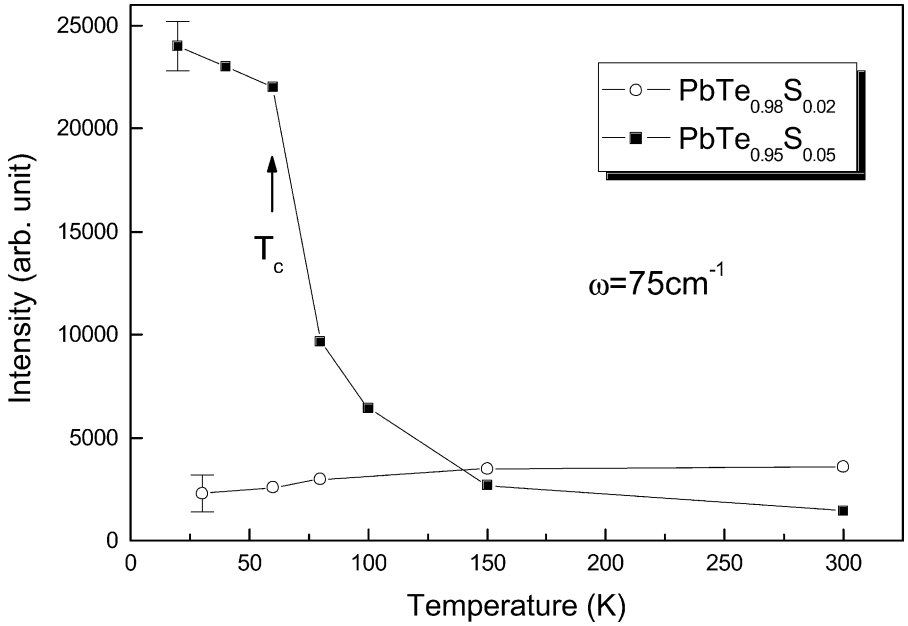

Fig. 7. Temperature dependence of the intensity of the mode at 75 cm^{-1}: (◯) $x = 0.02$; (■) $x = 0.05$.

mode in [0 0 1] direction. The phonon density of state of PbTe has a maximum at these frequencies [24]. Due to the temperature dependence of the mode intensity, we assume that it is the consequence of the already described off-center phenomena of sulphur in $PbT_{1-x}S_x$. At relatively high temperatures, the off-centers are randomly oriented, so the mode intensity connected with them is low. The off-center and electrical dipole ordering during the phase transition affect the crystal polarizability, and intensity of this mode increases. This kind of behaviour is stable above the temperature $T = 60$ K for the sample with $x = 0.05$, and further temperature decrease does not affect this mode intensity.

4. Conclusion

In this paper we analysed phonon properties of two samples of $PbTe_{1-x}S_x$: one with $x = 0.02$, where phase transition is not observed and the other with $x = 0.05$, where we confirmed the existence of a complex phase transition at $T = 60$ K.

The long wavelength optical phonon modes of these mixed crystals showed a two-mode behaviour. An additional mode at 75 cm^{-1} is induced by the off-center sulphur ions, and its intensity is strongly connected with the phase transition and the nature of these centers.

Acknowledgements

This work is supported by Serbian Ministry of Science, Technology and Development under project 1481.

References

[1] E.F. Steigmeier, G. Harbeke, Solid State Commun. (1970) 8.
[2] H. Kavamura, Proc. Third Int. Conf. Phys. Narrow-Gap Semiconductors, Warsaw, 1977, p. 7.
[3] S. Katayama, K. Murase, Solid State Commun. 36 (1980) 707.
[4] Q.T. Islam, B.A. Bunker, Phys. Rev. B 59 (1980) 2701.
[5] Kh.A. Abdulin, A.I. Lebedev, A.M. Gas'kov, V.N. Demin, V.P. Zlomanov, Pi'ma Zh. Eksp. Teor. Fiz. 40 (1984) 229 [JETP Lett. 40 (1984) 998].
[6] Kh.A. Abdulin, V.N. Demin, A.I. Lebedev, Fiz. Tverd. Tela. 28 (1986) 1020 [Sov. Phys. Solid State 28 (1986) 570].
[7] A.I. Dmitriev, G.V. Lashkarev, V.I. Litvinov, A.M. Gas'kov, N.V. Demin, Pis'ma Zh. Eksp. Teor. Fiz. 45 (1987) 304 [JETP Lett. 45 (1987) 383].
[8] A.I. Dmitriev, V.I. Lazorenko, V.I. Litvinov, G.V. Lashkarev, Pis'ma Zh. Eksp. Teor. Fiz. 47 (1988) 576 [JETP Lett. 47 (1988) 669].
[9] G. Hohler, Dynamical properties of IV–VI Compounds, Springer-Verlag, Berlin, 1983.
[10] Z. Vang, B.A. Bunker, Phys. Rev. B (1992) 46.
[11] A.N. Vasil'ev, Yu.P. Gaidukov, Uspehi Fiz. Nauk 141 (1983) 431.
[12] J. Trajić, M. Romčević, N. Romčević, S. Nikolić, A. Golubović, S. Đurić, V.N. Nikiforov, J. Alloys Comp. 365 (2004) 89.
[13] Yu.I. Ravich, B.A. Efimova, I.A. Smirnov, Semiconducting Lead Chalcogenides, Plenum, New York, 1970.
[14] J. van der Klink, S.N. Khanna, Phys. Rev. B 29 (1984) 2415.
[15] J.H. Cape, L.G. Hale, W.E. Tannent, Surf. Sci. 62 (1979) 639.
[16] J. Tang, A.C. Albrecht, Raman Spectroscopy, Plenum, New York, 1970.
[17] B.H. Henry, Raman Spectroscopy: Sixty Years On, Elsevier, Amsterdam, 1990.
[18] M. Kozielski, M. Szybowicz, F. Firszt, S. Legowski, H. Meczynska, J. Szatkowski, W. Paszkowicz, Cryst. Res. Technol. 34 (1999) 699.
[19] L. Genzel, T.P. Martin, C.H. Perry, Phys. Status Solidi (b) 62 (1974) 83.
[20] Y.S. Chen, W. Shoskley, G.L. Person, Phys. Rev. 151 (1966) 648.
[21] D.L. Peterson, A. Petrou, W. Giriat, A.K. Ramdas, S. Rodriguez, Phys. Rev. B 25 (1992) 10934.
[22] S. Venigopalan, A. Petrov, R.R. Galazka, A.K. Ramdas, S. Rodriguez, Phys. Rev. B 25 (1982) 2681.
[23] A.J. Sievers, Far infrared spectroscopy, Wiley, New York, 1971.
[24] W. Cochran, R.A. Cowley, G. Dolling, M.M. Elcombe, Proc. Roy. Soc. 293 (1966) 433.